



## The assessment of changes in the membrane surface during the filtration of wastewater treatment plant effluent

Edyta Kudlek\*, Mariusz Dudziak

*Faculty of Energy and Environmental Engineering, Silesian University of Technology, Konarskiego 18, 44-100 Gliwice, Poland, Tel. +48 32 237-24-78; email: edyta.kudlek@polsl.pl (E. Kudlek)*

Received 31 March 2018; Accepted 13 July 2018

---

### ABSTRACT

The physicochemical composition of water matrixes has a major impact on changes in the membrane surface properties (morphology, charge). In this research, this changes reflected in the obtained retention coefficient of micropollutants in the tested water matrixes. The conducted experiments indicated that the presence of inorganic compounds especially affected the carbamazepine retention ( $R = 97\%$ ) in the real effluent, beside the deionized water matrix ( $R = 99\%$ ). The blocking of the membrane surface by compounds present in real wastewater treatment plant effluent was only partially reversible. Whereas the filtration of the synthetic effluent had a beneficial impact on the volumetric permeate flux. The roughness analysis showed that the membrane surface was changing during the conducted filtration processes from homogeneous to a heterogeneous one. The atomic force microscopy images gave a good visualization of changes in the membrane topography and confirmed the occurrence of the fouling process during the filtration of solutions with a diversified physicochemical composition.

*Keywords:* Nanofiltration; Wastewater; Fouling; AFM images

---

### 1. Introduction

The nanofiltration (NF) is one of the pressure membrane processes, that are widely used in many applications, including pharmaceutical and personal care product industry, food industry, water and wastewater treatment [1–3]. They can also be used during technological water preparation [4].

The separation properties of membranes depend on the used membrane polymer, the nanocomposite additives [5], and the membrane preparation method. They all decide about the membrane surface roughness, size, shape, and form of the pores that make up the surface [6]. The micropollutants retention depends on the micro-hydrodynamic and interfacial events occurring at the membrane surface and in the membrane nanopores [7]. The size of most NF membrane pores is smaller than 2.0 nm [8]. Such nanoscale pore dimensions, in addition with charged functional groups occurring

on the whole surface and in the pores of the membrane, allow to retain charged solutes and/or solutes with a molecular weight below 200 Da [9].

During the NF, a co-existence of steric, Donnan, dielectric, and transport effects is observed [10]. In addition, it has been proven that different membranes have different susceptibility to adsorb compounds [11,12]. Many commercial NF membranes are multilayer membranes consisting of a microporous polysulfone support layer and a nonporous polyamide layer embedded on it [13]. Any change in the environmental conditions of the membrane, particularly changes in pH and ionic strength, may affect the conformation and the ionization of the polymer chains as well as the pore size of a membrane [14]. These changes affect the membrane permeability and the passage of molecules.

The selection of optimal operation parameters of the NF process must take into account the mitigation of the fouling phenomenon, which in general accompanies all membrane filtration techniques. The determination of the susceptibility

---

\* Corresponding author.

of membranes to the fouling process requires the examination of their surface using different advanced analytical techniques, including high resolution microscopy, spectroscopy with electromagnetic radiation, membrane surface charge measurements, and contact angles measurements.

Atomic force microscopy (AFM), along with scanning electron microscopy and transmission electron microscopy, are one of the most popular high-resolution microscopy techniques for imaging membrane surface [15]. The result of the AFM analysis is a three-dimensional scan of the tested membrane surface topography. The obtained image gives information about changes in the membrane morphology due to fouling phenomenon or chemical modification [16,17]. Kochkodan et al. [18] used the AFM method for the observation of changes in the surface roughness of unmodified commercial NF membranes and membranes after the modification with successive layers of poly-[(4-styrenesulfonic acid) co-(maleic acid)]. Guillen-Burrieza et al. [19] observed changes in the roughness of the polyvinylidene difluoride membrane caused by the scaling phenomenon. Changes caused by the organic and biofouling phenomenon can also be identified by AFM imaging [20,21].

AFM imaging can also provide information about the pore diameter and porosity of the membrane. However, the pore sizes estimated using this method may differ from those measured by porosimetry or membrane transport methods [22].

The paper presents the assessment of changes occurring on the membrane surface during the filtration process of various water matrices, including real wastewater from a wastewater treatment plant. A tubular polymer membrane was used for the research. In order to evaluate the separation properties of the membrane, the water matrices were spiked with pharmaceutical micropollutants from the group of psychoactive and nonsteroidal anti-inflammatory drugs. The analysis of the membrane surface morphology and roughness was performed using AFM. In addition, the change of membrane charge during the filtration of tested

water solutions was measured using the zeta potential measurement.

## 2. Material and methods

### 2.1. Material and reagents

The analytical standards of both, carbamazepine (CBZ), ibuprofen (IBU), and diclofenac (DCF) sodium salts of purity grade >97% were supplied by Sigma-Aldrich (Poland). The chemical characteristic of the tested compounds is presented in Table 1. Methanol and acetonitrile with over 99.5% of purity by Avantor Performance Materials Poland S.A. were also used in the investigations. Solid phase extraction (SPE) tubes Supelclean™ ENVI-8 were supplied by Sigma-Aldrich. The tubes were used for the determination of pharmaceutical concentration in the prepared water solutions. Dry nutrient broth and casein peptone by BTL Sp. z o.o. (Poland) and NH<sub>4</sub>Cl, NaCl, CaCl<sub>2</sub>·6H<sub>2</sub>O, MgSO<sub>4</sub>·7H<sub>2</sub>O, K<sub>2</sub>HPO<sub>4</sub>, KH<sub>2</sub>PO<sub>4</sub> by Avantor Performance Materials Poland S.A. were used for the preparation of the synthetic wastewater effluent.

### 2.2. NF process

The study on the changes in the membrane surface during the filtration of three water matrices was carried out using a polymeric NF membrane AFC80 by PCI Membrane System Inc. (USA) (Table 2). The membrane was placed in a tubular flow-through membrane module of a semi-industrial installation TMI 14 by J.A.M INOX Produkt (Poland). The total surface area of the membrane was 240 cm<sup>2</sup>. The filtration process was operated in a cross-flow mode with recirculation of the concentrate to the feeding tank (concentration mode) to collect 20% of the initial volume of the feed. The initial volume of the feed was 20 L. The process transmembrane pressure used in the study was 2.0 MPa. All used AFC80 membranes were subjected to conditioning by deionized water prior to

Table 1  
The structural and chemical characteristics of investigated compounds [23]

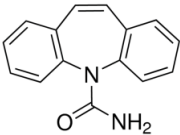
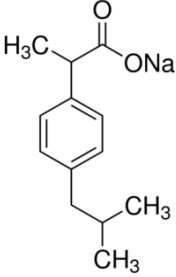
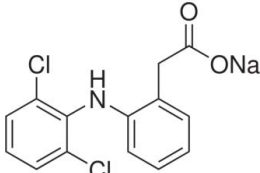
Compound	Carbamazepine	Ibuprofen sodium salt	Diclofenac sodium salt
Structural formula			
Molecular formula	C <sub>16</sub> H <sub>12</sub> N <sub>2</sub> O	C <sub>13</sub> H <sub>17</sub> O <sub>2</sub> Na	C <sub>14</sub> H <sub>10</sub> Cl <sub>2</sub> NNaO <sub>2</sub>
CAS No.	298-46-4	31121-93-4	15307-79-6
Molecular weight (Da)	236.3	228.26	318.13
Solubility in water (mg/L)	0.17	100	50
pK <sub>a</sub>	2.3	4.91	4.15
log K <sub>ow</sub>	2.45	3.97	4.51
Stokes radius (nm)	0.319	0.295	0.414

Table 2  
Characteristics of the used membrane (data from the membrane producer)

Membrane type	AFC80
Skin layer material	Polyamide
Molecular weight cut-off (Da)	<200
NaCl retention (%)	80
MgSO <sub>4</sub> retention (%)	98
pH range (-)	1.5–10.5
Hydrophilicity	4 <sup>a</sup>

<sup>a</sup>Hydrophilicity scale: 1 – low, 5 – high.

the main experiments. The filtration process for each tested water matrix was performed three times.

### 2.3. Water samples

The water matrices were prepared based on deionized water, a synthetic and a real effluent from a mechanical–biological wastewater treatment plant. The synthetic effluent was prepared according to the Polish Standard PN-72/C-04550.09 for raw synthetic municipal wastewater and diluted 10-fold to simulate 90% removal rate of all solution substrates. The real effluent was collected at a municipal wastewater treatment plant located in Upper Silesia (Poland). The water matrices were spiked with pharmaceutical micropollutants, that is, CBZ, IBU, and DCF sodium salts at a concentration of 1 mg/L. The pH of the deionized water matrix and the synthetic effluent was adjusted to 7 using 0.1 mol/L HCl or 0.1 mol/L NaOH. The physicochemical characteristics of tested water matrices are presented in Table 3.

### 2.4. Analytical procedure

The separation properties of the used membranes were evaluated based on the micropollutants retention coefficient (*R*) described in Eq. (1) as follows:

$$R = \left( 1 - \frac{C_p}{C_f} \right) \times 100\% \quad (1)$$

Table 3  
Physicochemical characteristics of tested water matrixes

Water matrix	Deionized water (1)	Synthetic effluent (2)	Real effluent (3)
pH	7.00	7.05	7.10
Conductivity (μS/cm)	2.00	998	1,058
Absorbance, λ = 254 nm (nm <sup>-1</sup> )	0.01	0.26	0.27
COD (mg O <sub>2</sub> /L)	–	48.54	49.87
BOD (mg O <sub>2</sub> /L)	–	5.12	5.01
TOC (mg/L)	5.02	34.98	35.14
IC (mg/L)	1.00	44.45	45.07

where *C<sub>p</sub>*, *C<sub>f</sub>* – micropollutant concentration in permeate and feed estimated after assumed filtration time (mg/L).

The retention coefficient was calculated after 15, 30, 45, 60, 75, 90, 105, 120, 135, 150, 165, and 180 min of filtration by the estimation of the micropollutants concentration in the feed/retentate mixture and the permeate. The concentrations of micropollutants were determined using high-performance liquid chromatography HPLC-UV by Varian (Poland) equipped with a Hypersil GOLD column by Thermo Scientific (USA) of length 25 cm, diameter 4.6 mm, and graining 5 μm. The chromatographic analysis was preceded by SPE of analyzed water samples. Details of the extraction method are presented in Ref. [24].

The volumetric permeate flux of deionized water (*J<sub>w</sub>*) and the tested water matrices (*J<sub>v</sub>*) was determined according to Eq. (2) as follows:

$$J_w, J_v = \frac{V}{F \times t} \quad (2)$$

where *J<sub>w</sub>*, *J<sub>v</sub>* – volumetric permeate flux (m<sup>3</sup>/m<sup>2</sup> s); *V* – permeate volume (m<sup>3</sup>); *F* – membrane surface area (m<sup>2</sup>); and *t* – filtration time (s).

The membrane surface blocking was defined by the relative permeability of membrane (*α<sub>v</sub>*) (Eq. (3)) as follows:

$$\alpha_v = \frac{J_v}{j_w} \quad (3)$$

The filtration of deionized water without micropollutants before and after the filtration of tested water matrices described by the relative deionized water flux (*α<sub>w</sub>*) (Eq. (4)), allowed for the examination of changes in transport properties of the membrane (fouling process).

$$\alpha_w = \left( \frac{J_{wp}}{J_w} \right) \times 100\% \quad (4)$$

where *J<sub>wp</sub>* – volumetric permeate flux for deionized water, estimated for the membrane after the filtration of the tested water matrices (m<sup>3</sup>/m<sup>2</sup> s).

The surface morphology and roughness changes of the membrane before and after the filtration of tested water matrices were analyzed using the AFM NTEGRA Prima from NT-MDT (Poland). The analyses were carried out using the time-lapse mode of AFM imaging. The obtained AFM pictures were analyzed by the NOVA 1.0.26.1644 software from NT-MDT (Poland).

Changes in the charge of the membrane surface were defined by the zeta potential (ζ) measured by the electrokinetic analyzer Surpass by Anton Paar (Switzerland). As an electrolyte, 0.01 mol/L KCl was used. pH was adjusted to be kept in that range from 2.5 to 8.0 using 0.1 mol/L HCl or 0.1 mol/L NaOH by Avantor Performance Materials Poland S.A. Measurements were carried out at 21°C.

## 3. Results and discussion

### 3.1. Separation properties of the membrane

The separation properties of the membrane were established according to the removal degrees of selected micropollutants.

Table 4 presents the obtained average retention coefficients of pharmaceutical micropollutants estimated during the 180 min of filtration. The retention of CBZ and DCF during the filtration of the deionized water based matrix exceeded 98%, whereas the concentration of IBU in the collected permeate decreased against the feed at about 88%. Retention coefficients of CBZ and DCF observed for the filtration of and real effluents were lower than ones noted for the deionized water matrix. The retention of CBZ did not exceed 97%. Only the retention of IBU increased during the filtration of the model and real effluent to over 90%.

The differences in the micropollutants retention coefficients observed for the tested water matrices resulted from the physicochemical composition of solutions. The presence of inorganic compounds in the feed affects the charge of the membrane surface [25]. Teixeira et al. [26] indicated that divalent  $\text{Ca}^{2+}$  cation adsorption on the membrane surface reduced its negative charge. Whereas, if the feed contains both, divalent cations ( $\text{Mg}^{2+}$ ) and anions ( $\text{SO}_4^{2-}$ ), the negative charge reducing effect of the cations is blocked by divalent anions [27]. The conducted zeta potential measurements confirmed the significant influence of the composition of the filtered water matrix on the change of the membrane charge (Fig. 1).

Table 4  
Micropollutant retention coefficient

Water matrix	Parameter	Value (%)
Water matrix 1 (deionized water)	$R_{\text{CBZ}}$	$99.44 \pm 0.05$
	$R_{\text{IBU}}$	$88.05 \pm 0.01$
	$R_{\text{DCF}}$	$98.57 \pm 0.25$
Water matrix 2 (synthetic effluent)	$R_{\text{CBZ}}$	$96.59 \pm 0.12$
	$R_{\text{IBU}}$	$90.13 \pm 0.10$
	$R_{\text{DCF}}$	$96.24 \pm 0.32$
Water matrix 3 (real effluent)	$R_{\text{CBZ}}$	$96.94 \pm 0.10$
	$R_{\text{IBU}}$	$91.02 \pm 0.05$
	$R_{\text{DCF}}$	$96.80 \pm 0.30$

The results presented in Fig. 1. are the arithmetic average of the three replicates of each experiment. For all cases, assigned error (estimated based on the standard deviation) did not exceed 5%, so the results are presented without marking of the error range.

The zeta potential of the membrane surface in the tested range of pH from 2.5 to 8.0 indicated on a negative charge of the membrane. The membrane showed only a positive charge during the filtration of deionized water with pH below 4. All experiments conducted in this study were focused on water solutions, pH of which was adjusted to about 7.0. In this pH level the most negative charge of the membrane surface was observed for deionized water. The filtration of the synthetic effluent (water matrix 2), which was prepared on the basis of tap water and dry nutrient broth, casein peptone,  $\text{NH}_4\text{Cl}$ ,  $\text{NaCl}$ ,  $\text{CaCl}_2 \cdot 6\text{H}_2\text{O}$ ,  $\text{MgSO}_4 \cdot 7\text{H}_2\text{O}$ ,  $\text{K}_2\text{HPO}_4$  and  $\text{KH}_2\text{PO}_4$  resulted in the smallest change of the membrane charge. However, the measured zeta potential for this membrane was still about  $-23$  mV. The obtained results confirmed that the presence of several ions in the feed had a major impact on the charge of the membrane during the filtration process.

### 3.2. Control of the volumetric permeate flux

Fig. 2 presents the volumetric permeate flux of deionized water and the tested water matrices for the AFC80 membrane during the filtration. The highest calculated permeate flux was observed for the synthetic wastewater. The average value of this parameter was  $10.65 \times 10^{-6} \text{ m}^3/\text{m}^2/\text{s}$ . The lowest volumetric permeate flux was estimated during the filtration of the real wastewater plant effluent (water matrix 3). During the first 45 min of its filtration, a significant decrease of the volumetric permeate flux from  $9.95 \times 10^{-6}$  to  $9.64 \times 10^{-6} \text{ m}^3/\text{m}^2/\text{s}$  was observed. The continuation of the filtration process allowed for the stabilization of the  $J_v$  value at the level of  $9.66 \times 10^{-6} \text{ m}^3/\text{m}^2/\text{s}$ . The observed differences in the values of the volumetric permeate fluxes between the tested water matrices were not significant. The value of the deviation of the average permeate flux of individual water matrices with respect to the volumetric permeate flux of deionized water

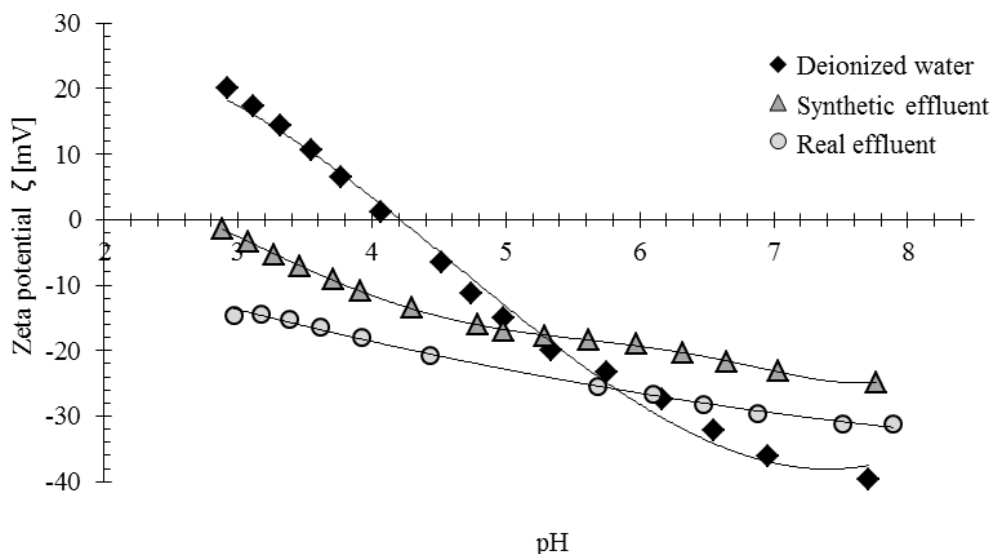


Fig. 1. Changes in the zeta potential of the membrane surface after the filtration of water matrices.

determined during the conditioning of the membrane did not exceed 10%. The relatively small, but noticeable differences could be due to the fact, that new membrane samples were used for each individual experiment. These membranes often have a slightly different characteristics.

The observation of changes in the volumetric permeate flux during the filtration of all tested water matrices allowed for the calculation of the relative permeability of the membrane ( $\alpha_v$ ). The comparison of the volumetric permeate flux for deionized water, estimated for the membrane before and after the filtration of the tested water matrices, set the value of the relative deionized water flux ( $\alpha_w$ ) (Table 5).

Based on both the deionized water matrix and synthetic effluent volumetric permeate flux values and the calculated relative permeability of membrane, it can be concluded that the phenomenon of membrane blocking did not occur. A contrary dependence, related with the increase in membrane permeability was observed. The  $\alpha_v$  calculated during the filtration of both water matrices was higher than 1.0, which indicated on a favorable change in the hydraulic capacity of the used membrane. Only in the case of the real effluent filtration, the  $\alpha_v$  was below 1.0. As previously stated, the decrease in the volumetric permeate flux of the real effluent could be associated with the fouling phenomenon caused by the deposition of high-molecular weight organic substances and other inorganic compounds on the membrane surface. The blocking of the membrane surface by the compounds present in the feed was only partially reversible. The recovery of

Table 5  
Characteristic of the permeate fluxes

Water matrix	Parameter	Value
Water matrix 1	$\alpha_v$	1.03
	$\alpha_w$ (%)	100
Water matrix 2	$\alpha_v$	1.06
	$\alpha_w$ (%)	106
Water matrix 3	$\alpha_v$	0.97
	$\alpha_w$ (%)	99

deionized water flux ( $\alpha_w$ ) determined after filtration of the tested real effluent was 99%. The  $\alpha_w$  estimated after the filtration of the synthetic wastewater effluent exceeded 100%. It indicates a permanent change in the hydraulic permeability of the membrane.

### 3.3. Analysis of the membrane surface

In order to assess the changes occurred on the surface of the membrane, representative membrane fragments were subjected to AFM analysis. The results of the membrane roughness analysis are summarized in Table 6 and shown graphically in Fig. 3.

Based on the root mean square ( $Rq$ ) and surface kurtosis of the membrane ( $S_{ku}$ ), which is a measure of the flattening

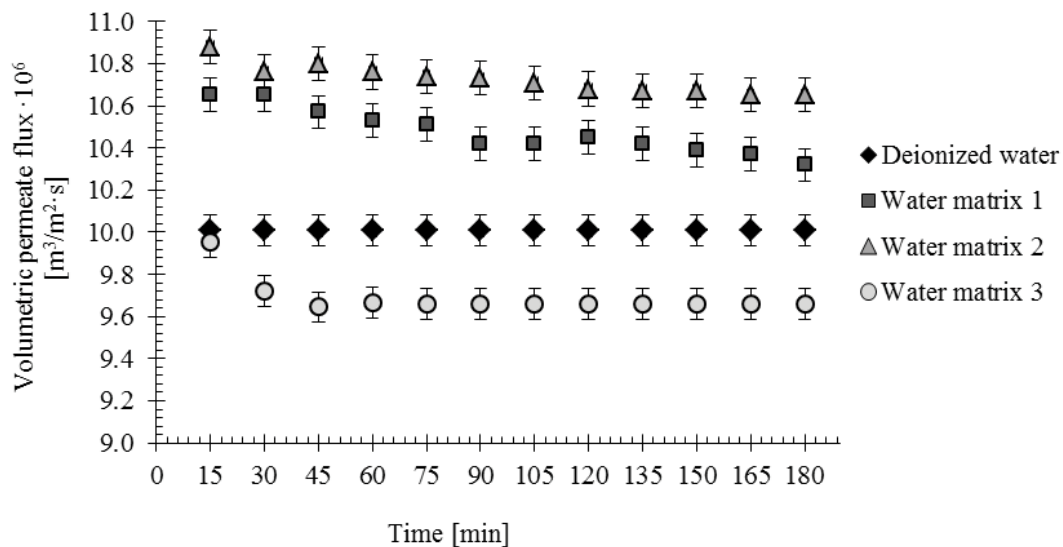


Fig. 2. Changes in the volumetric permeate flux during the filtration of water matrices.

Table 6  
Results of the membrane roughness analysis

Type of membrane	Root mean square $Rq$ (nm)	Maximum peak (nm)	Surface skewness $S_{sk}$	Surface kurtosis $S_{ku}$
New membrane	13	164	0.67	2.30
After filtration of water matrix 1	19	260	1.70	10.01
After filtration of water matrix 2	43	593	1.87	6.73
After filtration of water matrix 3	150	940	2.23	4.71

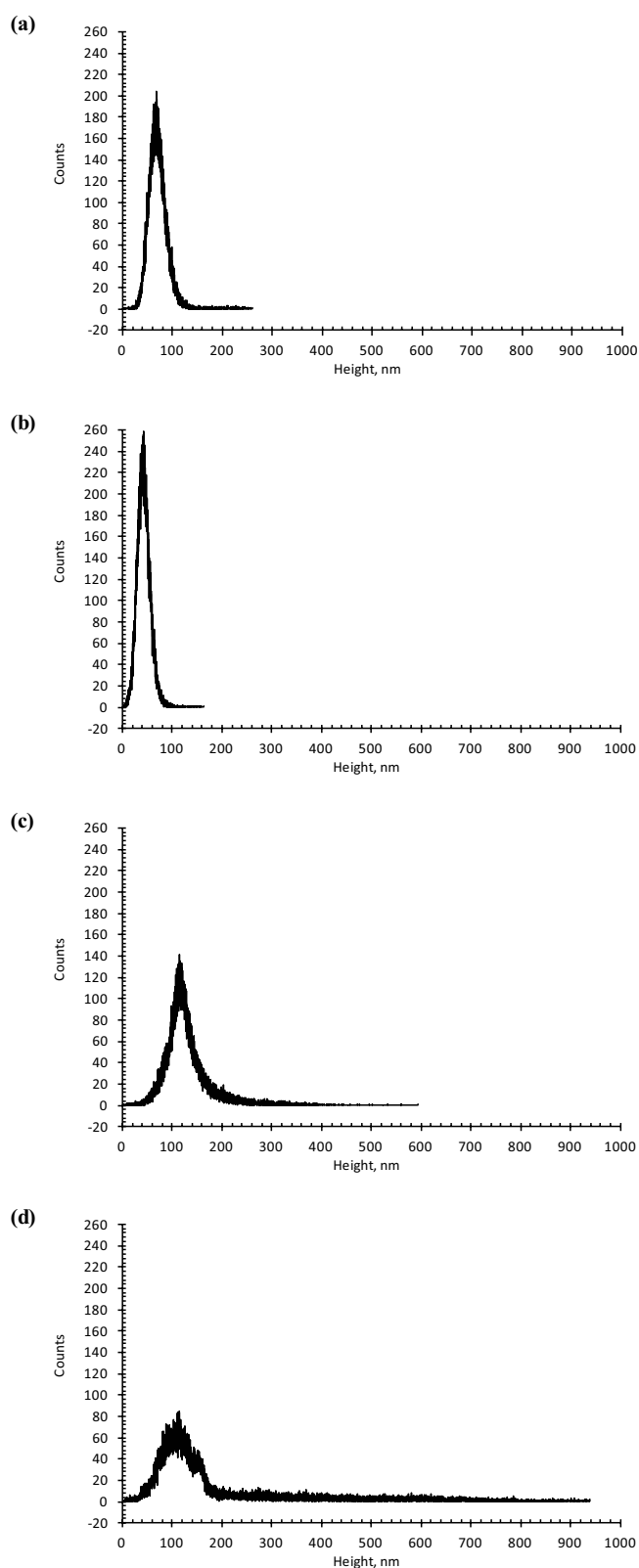


Fig. 3. Roughness analysis histograms of (a) a new membrane and membranes after the filtration of (b) deionized water, (c) synthetic effluent, and (d) real effluent.

of the surface compared with the Gaussian normal distribution, the surface of the AFC80 membrane was considered as homogeneous.  $S_{ku}$  values below 3.0 are characteristic for smooth surfaces. During the filtration of deionized water based matrix, no clear changes in the surface roughness were observed. However, the value of membrane surface skewness ( $S_{sk}$ ) assumed during the filtration of all tested water matrices values exceeded 1.0 that is typical for areas with many hills. The increase of the  $S_{sk}$  was related to the deposition of micropollutants and other contaminants present especially in the synthetic and real effluent, in the valleys of the new membrane. The topography of the postprocessed membranes changed its type to heterogeneous ones. This was also confirmed by the surface kurtosis increase.

Most significant changes in the morphology of the NF membranes were observed during the filtration of the synthetic and real wastewater treatment plant effluent. The root mean square increased from 13 nm for a new membrane to 43 nm for the membrane after the synthetic effluent filtration and 150 nm for the membrane after the real effluent filtration, respectively. Histograms of the roughness analysis (Fig. 2) show that the height of most peaks distributed on the membrane skin layer ranged from 60 to 180 nm. The highest identified peak after the filtration of the real effluent reached 940 nm. Whereas the surface of a new membrane or a membrane after the filtration of the deionized water based matrix was covered with peaks ranged mainly to 100 nm.

According to Hirose et al. [28], the surface unevenness of membranes increases their effective membrane area. Rough surfaces made from the same material present more adsorption area than smooth surfaces [29]. Thus, rough membranes should characterize with a higher retention of removed compounds. This relationship was observed only in the case of IBU retention, which increased with the membrane roughness.

The accumulation of compounds occurring in the feed in the “valleys” of the membrane surface resulted in “valley clogging.” It can be assumed that this phenomenon was responsible for the irreversible fouling process during the filtration of the real wastewater treatment plant effluent. On the other hand, high roughness of NF membranes can also reduce the fouling process by creating micro- or nanoturbulences on the membrane surface that lead to the increase of the mass transfer coefficient [30].

In Fig. 4, images of the membrane skin layer obtained before and after filtration of tested water matrices are compared. They show representative membrane areas of  $10 \times 10 \mu\text{m}^2$ .

The AFM images are a good visualization of changes in the membrane surface topography. They confirmed the occurrence of the fouling process during the filtration of the real wastewater treatment plant effluent. It should be emphasized that during the filtration of this complex matrix, the low- and high-molecular-weight compounds formed bunch structures that covered the entire surface of the membrane (Fig. 3(d)). These bunch structures created a so-called “secondary membrane” on the membrane surface. The formed new layer contributes to the change in the retention properties of the membrane against organic micropollutants [31].



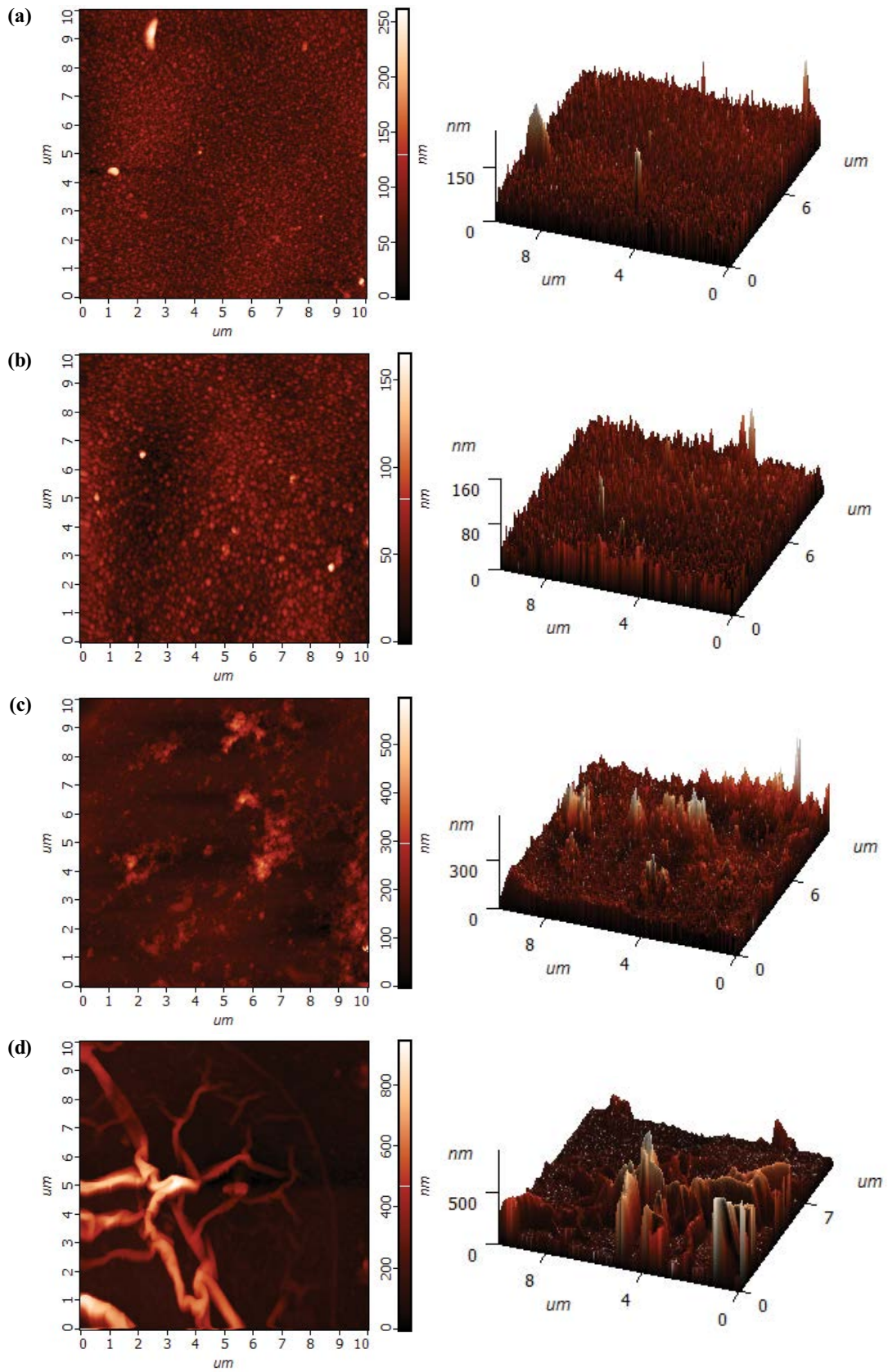


Fig. 4. AFM images of the surface of (a) a new membrane and membranes after the filtration of (b) deionized water, (c) synthetic effluent, and (d) real effluent.

#### 4. Conclusions

The conducted investigations indicated that the physico-chemical composition of the feed had a major impact on the changes in the tested membrane surface charge. The membrane charge is one of the factors determining the retention capacity of the membrane. The presence of inorganic and organic compounds in the synthetic and real treatment plant effluent decreased the retention of CBZ and DCF. An adverse relationship was observed in the case of IBU retention coefficient, which reached 91% during the filtration of the real effluent. It was also noted that the blocking of the membrane surface by compounds present in real wastewater treatment plant effluent was only partially reversible. Whereas the filtration of the synthetic effluent had a beneficial impact on the volumetric permeate flux. The conducted roughness analysis showed that the membrane surface was changing during the filtration processes from a homogeneous to a heterogeneous one. The samples of the membrane after the filtration of the real effluent were covered by bunch structures, which was detected during the AFM imaging. These structures were responsible for the fouling process and the change in the membrane retention properties.

#### Acknowledgment

This work was supported by Ministry of Science and Higher Education Republic of Poland within statutory funds.

#### References

- [1] Z.-Q. Yan, L.-M. Zeng, Q. Li, T.-Y. Liu, H. Matsuyama, X.-L. Wang, Selective separation of chloride and sulfate by nanofiltration for high saline wastewater recycling, *Sep. Purif. Technol.*, 166 (2016) 135–141.
- [2] Z. Chen, J. Luo, Y. Wang, W. Cao, B. Qi, Y. Wan, A novel membrane-based integrated process for fractionation and reclamation of dairy wastewater, *Chem. Eng. J.*, 313 (2017) 1061–1070.
- [3] D.L. Oatley-Radcliffe, M. Walters, T.J. Ainscough, P.M. Williams, A.W. Mohammad, N. Hilal, Nanofiltration membranes and processes: a review of research trends over the past decade, *J. Water Process Eng.*, 19 (2017) 164–171.
- [4] Cs.Zs. Torma, E. Cséfalvay, Nanofiltration: a final step in industrial process water treatment, *Period. Polytech. Chem. Eng.*, 62 (2018) 68–75.
- [5] E. Bet-Moushoul, Y. Mansourpanah, K. Farhadi, M. Tabatabaei, TiO<sub>2</sub> nanocomposite based polymeric membranes: a review on performance improvement for various applications in chemical engineering processes, *Chem. Eng. J.*, 283 (2016) 29–46.
- [6] S.T. Muntha, A. Kausar, M. Siddiq, Advances in polymeric nanofiltration membrane: a review, *Polymer Plast. Technol. Eng.*, 56 (2017) 841–856.
- [7] A.W. Mohammad, Y.H. Teow, W.L. Ang, Y.T. Chung, D.L. Oatley-Radcliffe, N. Hilal, Nanofiltration membranes review: recent advances and future prospects, *Desalination*, 356 (2015) 226–254.
- [8] Z. Chen, J. Luo, X. Hang, Y. Wan, Physicochemical characterization of tight nanofiltration membranes for dairy wastewater treatment, *J. Membr. Sci.*, 547 (2018) 51–63.
- [9] J. Lin, C.Y. Tang, C. Huang, Y.P. Tang, W. Ye, J. Li, J. Shen, R. Van den Broeck, J. Van Impe, A. Volodin, C. Van Haesendonck, A. Sotito, P. Luis, B. Van der Bruggen, A comprehensive physico-chemical characterization of superhydrophilic loose nanofiltration membranes, *J. Membr. Sci.*, 501 (2016) 1–14.
- [10] T.-Y. Liu, L.-X. Bian, H.-G. Yuan, B. Pang, Y.-K. Lin, Y. Tong, B. Van der Bruggen, X.-L. Wang, Fabrication of a high-flux thin film composite hollow fiber nanofiltration membrane for wastewater treatment, *J. Membr. Sci.*, 478 (2015) 25–36.
- [11] A.I. Schäfer, I. Akanyeti, A.J.C. Semião, Micropollutant sorption to membrane polymers: a review of mechanisms for estrogens, *Adv. Colloid Interface Sci.*, 164 (2011) 100–117.
- [12] A.J.C. Semião, A.I. Schäfer, Removal of adsorbing estrogenic micropollutants by nanofiltration membranes. Part A – Experimental evidence, *J. Membr. Sci.*, 431 (2013) 244–256.
- [13] C.Y. Tang, Y.-N. Kwon, J.O. Leckie, Effect of membrane chemistry and coating layer on physicochemical properties of thin film composite polyamide RO and NF membranes: I. FTIR and XPS characterization of polyamide and coating layer chemistry, *Desalination*, 242 (2009) 149–167.
- [14] J. Luo, Y. Wan, Effects of pH and salt on nanofiltration – a critical review, *J. Membr. Sci.*, 438 (2013) 18–28.
- [15] D.J. Johnson, D.L. Oatley-Radcliffe, N. Hilal, State of the art review on membrane surface characterisation: visualisation, verification and quantification of membrane properties, *Desalination*, 434 (2018) 12–36.
- [16] D. Johnson, S. Al Malek, B. Al-Rashdi, N. Hilal, Atomic force microscopy of nanofiltration membranes: effect of imaging mode and environment, *J. Membr. Sci.*, 389 (2012) 486–498.
- [17] A. Matin, H. Shafi, Z. Khan, M. Khaled, R. Yang, K. Gleason, F. Rehman, Surface modification of seawater desalination reverse osmosis membranes: characterization studies & performance evaluation, *Desalination*, 343 (2014) 128–139.
- [18] V. Kochkodan, Y. Manawi, D. Johnson, A. Kayvani Fard, M. Atieh, Surface modification of polyamide membranes using the layer-by-layer technique: characterization and antifouling potential, *Desal. Wat. Treat.*, 69 (2017) 84–92.
- [19] E. Guillen-Burrieza, R. Thomas, B. Mansoor, D. Johnson, N. Hilal, H. Arafat, Effect of dry-out on the fouling of PVDF and PTFE membranes under conditions simulating intermittent seawater membrane distillation (SWMD), *J. Membr. Sci.*, 438 (2013) 126–139.
- [20] N. Park, B. Kwon, I.S. Kim, J. Cho, Biofouling potential of various NF membranes with respect to bacteria and their soluble microbial products (SMP): characterizations, flux decline, and transport parameters, *J. Membr. Sci.*, 258 (2005) 43–54.
- [21] D. Johnson, F. Galiano, S.A. Deowan, J. Hoinkis, A. Figoli, N. Hilal, Adhesion forces between humic acid functionalized colloidal probes and polymer membranes to assess fouling potential, *J. Membr. Sci.*, 484 (2015) 35–46.
- [22] M. Khayet, C. Feng, K. Khulbe, T. Matsuura, Preparation and characterization of polyvinylidene fluoride hollow fiber membranes for ultrafiltration, *Polymer*, 43 (2002) 3879–3890.
- [23] S. Kim, P.A. Thiessen, E.E. Bolton, J. Chen, G. Fu, A. Gindulyte, L. Han, J. He, S. He, B.A. Shoemaker, J. Wang, B. Yu, J. Zhang, S.H. Bryant, PubChem substance and compound databases, *Nucleic Acids Res.*, 4 (2016) D1202–D1213.
- [24] J. Bohdziewicz, E. Kudlek, M. Dudziak, Influence of the catalyst type (TiO<sub>2</sub> and ZnO) on the photocatalytic oxidation of pharmaceuticals in the aquatic environment, *Desal. Wat. Treat.*, 57 (2016) 1552–1563.
- [25] N. Hilal, A.F. Ismail, T. Matsuura, D. Oatley-Radcliffe, *Membrane Characterization*, Elsevier B.V., Amsterdam, 2017.
- [26] M.R. Teixeira, M.J. Rosa, M. Nyström, The role of membrane charge on nanofiltration performance, *J. Membr. Sci.*, 265 (2005) 160–166.
- [27] A.E. Childress, M. Elimelech, Effect of solution chemistry on the surface charge of polymeric reverse osmosis and nanofiltration membranes, *J. Membr. Sci.*, 119 (1996) 253–268.
- [28] M. Hirose, H. Ito, Y. Kamiyama, Effect of skin layer surface structures on the flux behaviour of RO membranes, *J. Membr. Sci.*, 121 (1996) 209–215.
- [29] A.L. Carvalho, F. Mauger, V. Silva, A. Hernández, L. Palacio, P. Pradanos, AFM analysis of the surface of nanoporous membranes: application to the nanofiltration of potassium clavulanate, *J. Mater. Sci.*, 46 (2011) 3356–3369.
- [30] P. Izák, M.H. Godinho, P. Brogueira, J.L. Figueirinhas, J.G. Crespo, 3D topography design of membranes for enhanced mass transport, *J. Membr. Sci.*, 321 (2008) 337–343.
- [31] D. Dolar, A. Vuković, D. Asperger, K. Kosutić, Effect of water matrices on removal of veterinary pharmaceuticals by nanofiltration and reverse osmosis membranes, *J. Environ. Sci. (China)*, 23 (2011) 1299–1307.